DOI: 10.1534/genetics.108.091314

The *multiple-wing-hairs* Gene Encodes a Novel GBD–FH3 Domain-Containing Protein That Functions Both Prior to and After Wing Hair Initiation

Jie Yan,*[,1] David Huen,[†,1] Terri Morely,[†] Glynnis Johnson,[†] David Gubb,[2] John Roote[†] and Paul N. Adler*[,3]

[†]*Department of Genetics, University of Cambridge, Cambridge CB2 3EH, United Kingdom and* *Biology Department, Department of Cell Biology, Morphogenesis and Regenerative Medicine Institute and Cancer Center, University of Virginia, Charlottesville, Virginia 22903*

Manuscript received May 12, 2008
Accepted for publication June 27, 2008

ABSTRACT

The *frizzled* signaling/signal transduction pathway controls planar cell polarity (PCP) in both vertebrates and invertebrates. Epistasis experiments argue that in the Drosophila epidermis *multiple wing hairs* (*mwh*) acts as a downstream component of the pathway. The PCP proteins accumulate asymmetrically in pupal wing cells where they are thought to form distinct protein complexes. One is located on the distal side of wing cells and a second on the proximal side. This asymmetric protein accumulation is thought to lead to the activation of the cytoskeleton on the distal side, which in turn leads to each cell forming a single distally pointing hair. We identified *mwh* as CG13913, which encodes a novel G protein binding domain–formin homology 3 (GBD–FH3) domain protein. The Mwh protein accumulated on the proximal side of wing cells prior to hair formation. Unlike planar polarity proteins such as Frizzled or Inturned, Mwh also accumulated in growing hairs. This suggested that *mwh* had two temporally separate functions in wing development. Evidence for these two functions also came from temperature-shift experiments with a temperature-sensitive allele. Overexpression of Mwh inhibited hair initiation, thus Mwh acts as a negative regulator of the cytoskeleton. Our data argued early proximal Mwh accumulation restricts hair initiation to the distal side of wing cells and the later hair accumulation of Mwh prevents the formation of ectopic secondary hairs. This later function appears to be a feedback mechanism that limits cytoskeleton activation to ensure a single hair is formed.

THE epidermis of many animals is polarized within the plane of the tissue. This tissue planar cell polarity (PCP) is dramatic in the adult cuticle of Drosophila, which is decorated with parallel arrays of hairs and sensory bristles. PCP in Drosophila is under the control of the *frizzled* (*fz*) signaling pathway (Gubb and García-Bellido 1982; Vinson and Adler 1987; Lawrence *et al.* 2007) and in recent years it has become clear that this pathway also controls planar polarity during vertebrate gastrulation, during the differentiation of stereocilia in the inner ear, and in the mammalian epidermis (Jessen *et al.* 2002; Wallingford *et al.* 2002; Curtin *et al.* 2003; Guo *et al.* 2004; Dabdoub and Kelley 2005; Montcouquiol *et al.* 2006; Wang *et al.* 2006; Ybot-Gonzalez *et al.* 2007).

In the fly wing *fz* pathway genes have been placed into three groups that represent both phenotypic and epistasis groups (Adler 1992; Wong and Adler 1993). These are the PCP (or core) genes, the planar polarity effector (PPE) genes, and the *multiple-wing-hairs* (*mwh*) gene. The PCP group includes *fz*, *disheveled* (*dsh*), *prickle/spiny leg* (*pk/sple*), *Van Gogh* (*Vang*) (aka *strabismus*), *starry night* (*stan*) (aka *flamingo*), and *diego* (*dgo*). The protein products of these genes accumulate asymmetrically on the distal (Fz, Dsh, and Dgo), proximal (Vang and Pk), or both distal and proximal (Stan) sides of wing cells (Usui *et al.* 1999; Axelrod 2001; Strutt 2001; Tree *et al.* 2002; Bastock *et al.* 2003; Das *et al.* 2004). These genes/proteins act as a functional group and are co-requirements for the asymmetric accumulation of the others. Mutations in PCP genes result in the hair forming at a central location on the apical surface of wing cells and pointing in an abnormal direction (Wong and Adler 1993).

The PPE group includes *inturned* (*in*), *fuzzy* (*fy*), and *fritz* (*frtz*). Mutations in these genes differ from those in PCP genes as many mutant wing cells form two or three hairs with abnormal polarity. These hairs initiate at abnormal locations along the cell periphery. Several observations argue that the PPE genes function downstream of the PCP genes. First, loss-of-function mutations in PPE genes are epistatic to both gain and loss of

[1]These authors contributed equally to this work.

[2]CIC Biogune, Parque Technológico de Bizkaia 801A, Derio 48160, Spain.

[3]*Corresponding author:* Biology Department, Gilmer Hall, University of Virginia, Charlottesville, VA 22903. E-mail: pna@virginia.edu

functions in PCP genes (Lee and Adler 2002; Wong and Adler 1993). Next, the function of the PPE genes is not required for the asymmetric accumulation of PCP proteins (Usui *et al.* 1999; Axelrod 2001; Feiguin *et al.* 2001; Strutt 2001; Bastock *et al.* 2003). Finally, the In protein has been found to accumulate on the proximal side of wing cells under the direction of the PCP genes (Adler *et al.* 2004).

The *multiple-wing-hairs* (*mwh*) gene is the sole member of the third group. Mutations in *mwh* are epistatic to mutation in both the PCP and PPE genes (Lee and Adler 2002; Wong and Adler 1993) and *mwh* is not required for the asymmetric accumulation of PCP or PPE proteins (Usui *et al.* 1999; Axelrod 2001; Strutt 2001; Adler *et al.* 2004). Hence, *mwh* is thought to be the most downstream gene. A typical *mwh* wing cell produces three to five hairs with abnormal polarity and in this way differs from the upstream genes. Often some of the hairs produced by *mwh* cells are quite small. As is the case for PPE mutant cells, *mwh* cells form hairs at abnormal locations along the cell periphery (Wong and Adler 1993). Strikingly the abnormal polarity patterns seen in the wings of mutants are not random (Gubb and García-Bellido 1982; Wong and Adler 1993). Rather, the patterns are similar from one wing to another and similar for mutations in the PCP, PPE, and *mwh* genes providing additional evidence that these genes all function together in the generation of PCP (Taylor *et al.* 1998).

Studies on *mwh* have been limited due to the gene not having been characterized molecularly. We report here that *mwh* is CG13913, which encodes a novel G protein binding domain–formin homology 3 (GBD–FH3) domain protein. The expression of *mwh* mRNA increases prior to hair initiation (Ren *et al.* 2005) and we confirmed that this was also the case for Mwh protein. During this early period the protein accumulated on the proximal side of wing cells in a punctate manner. Overexpression of Mwh led to a delay in hair initiation, consistent with Mwh functioning as an antagonist of the cytoskeleton. Hence, we argue the proximal accumulation restricted hair initiation to the distal side of wing cells. Unlike other *fz* pathway proteins Mwh accumulated in growing hairs. Shift experiments with a temperature-sensitive allele showed that *mwh* functioned after hair initiation to inhibit the formation of secondary hairs. Our data point to *mwh* having two functions. We hypothesize an early Mwh function that controls hair polarity and a later one that prevents the formation of secondary hairs. We suggest that Mwh in and in the vicinity of growing hairs mediates the inhibition of secondary hair initiation.

MATERIALS AND METHODS

Fly genetics: All flies were raised at 25° unless otherwise stated. Mutant stocks were obtained from the Drosophila Stock Center at Indiana University, generated in our lab, or were generous gifts from J. Axelrod, D. Strutt, T. Uemura, and T. Wolff. The FLP/FRT technology was used to generate genetics mosaics. To direct transgene expression, we used the Gal4/UAS system. For temperature-shift experiments the relevant animals were collected as white prepupae, placed into fresh food vials, and moved to the proper incubator. In line with FlyBase usage we use *starry night* instead of *flamingo* and *Van Gogh* instead of *strabismus*.

Immunostaining: A standard staining procedure was used (Adler *et al.* 2004). Briefly, tissues were fixed with formaldehyde, rinsed, incubated with primary antibody, rinsed, incubated with flourescently labeled secondary antibody, and then mounted in ProLong (Invitrogen) Gold mountant.

Plasmid Constructs: *mwh cloning:* PCR, cloning, and sequencing used standard protocols. RACE was performed with a Marathon kit (Clontech). The extended mwh cDNA was PCR amplified with an Expand kit (Boehringer) and cloned into pCR2.1 (Clontech). pUASt-*mwh* was prepared by excising the *mwh* insert from pCR2.1 with *Eco*RI and cloning it into the *Eco*RI site of pUASt.

mwh subcloning for protein expression: The *mwh* EST clone SD18376 was used as the template. The last exon of *mwh* with correct coding frame was amplified with primers GATE-mwh5: GGGGACAAGTTTGTACAAAAAAGCAGGCTTCTTTCTCAA CACGTTCATTGAG-AGCG and GATE-mwh3: GGGGACCAC TTTGTACAAGAAAGCTGGGTCTTAGTAGAGG-CCGGATG GCAGA. The PCR product was subcloned into pDORN 221 vector and then subcloned into pDEST 17 vector (Invitrogen Gateway technology).

Antibodies: His-tagged truncated Mwh proteins (encoded by last exon) were expressed in *Escherichia coli* BL21-AI cells (Invitrogen) using the DEST 17 vector and purified from inclusion bodies (Novagen). Antibodies against Mwh were raised in rats and rabbits. Monoclonal anti-Armadillo and anti-Flamingo antibodies were obtained from Developmental Studies Hybridoma Bank at the University of Iowa. Alexa 488- and Alexa 568-conjugated secondary antibodies were purchased from Molecular Probes. Alexa 568 and 647 phalloidin were purchased from Molecular Probes.

RESULTS

CG13913 is *mwh*: We identified *mwh* by deficiency mapping followed by sequencing of candidate genes. We identified mutations in CG13913 in four null alleles of *mwh*, all of which would truncate the protein (Table 1). These included two mutations in splice acceptor sites, one nonsense mutation, and one small deletion that altered the reading frame. For the mwh^{1} allele, which is a phenotypic null we were unable to amplify the 3′ end of the gene, suggesting it might be associated with a deletion, but we did not obtain definitive evidence on this point. By immunostaining we did not detect any Mwh protein in mwh^{1} mutant cells, consistent with it being a null allele. In our collection of *mwh* alleles there is a single hypomorphic allele (mwh^{6}) and we found it contained a change of Cys 222 to Tyr. The significance of this change will be discussed further below. By RACE analysis we confirmed that CG13913 was internally spliced as predicted and that there was a noncoding exon encoded by sequences some 20 kb upstream of the CG13913 coding exons (Figure 1A).

TABLE 1

Nature of *mwh* mutations

Allele	Molecular change	Phenotype	Comment
mwh^{1}	Uncertain, unable to amplify 3′ end of gene	Null	Likely a deletion, no CRM
mwh^{2}	C1229633T	Null	Stop at codon 11
mwh^{3}	G1230259T	Null	Eliminates exon 5 splice acceptor
mwh^{4}	1230897–1230902 deletion	Null	Deletes exon 7 splice acceptor
mwh^{5}	1230570–1230582 deletion	Null	Changes reading frame after codon 243 followed by 39 novel amino acids prior to a stop codon
mwh^{6a}	G1230445A	Hypomorphic, ts	Cys 222 Tyr

[a]The temperature-sensitive (ts) *mwh*^{6} allele contained three amino acid substitutions compared to the reference wild-type sequence; however two of these were also found on another chromosome (from the same parental stock) that did not show the *mwh*^{6} phenotype and hence are likely neutral polymorphisms.

Several lysozyme genes exist in both orientations within the large CG13913 first intron.

Additional proof that CG13913 was *mwh* came from experiments where we found that a *UAS-CG13913* transgene provided rescue of a null *mwh* allele when driven by either *apterous-Gal4* (*ap-Gal4*) or *engrailed-Gal4* (Figure 1, C and D). Almost complete rescue was obtained using the *actin-Gal4* driver, which drives expression at a somewhat lower level. In contrast, little rescue was obtained using *patched-Gal4* (*ptc-Gal4*) and this was restricted to very proximal parts of the *ptc* domain (data not shown). As is described later, this is presumably due to *ptc-Gal4* not being effective in driving *mwh* expression just prior to and during hair morphogenesis.

Independent evidence that CG1913 was *mwh* came from our finding that three separate transformants (41513, 41514, and 45265) from the Vienna Drosophila RNAi Center that encoded double-stranded RNA from CG13913 produced a *mwh* mutant phenotype when expressed by *ap-GAL4*. These data provided compelling evidence that *CG13913* encoded *mwh*. Henceforth we refer to CG13913 as *mwh*.

The Mwh protein: The predicted Mwh ORF encodes an 836 residue protein with a formin FH3 and GBD (GTPase binding domain) domains (Figure 1B). These two domains are frequently found together in proteins such as the Diaphanous family formins. In some recent papers these "sequence domains" have been renamed to reflect "structural domains" as a GBD (smaller than previous GBD domain), a Dad interacting domain (DID), corresponding to part of both the older GBD and FH3 domains), and a dimerization domain (DD), corresponding to part of the older FH3 domain) domain (Goode and Eck 2007). These domains correspond to the regulatory region of Diaphanous family formins.

We identified Mwh homologs in other arthropods, including the lepidopteran *Bombyx mori*, the coleopteran *Tribolium castaneum*, the hemipteran *Pediculus humanus*, the hymenopteran *Apis melifera*, and even the crustacean *Daphnia pulex* (see alignments in supplemental Figure S1). However it was not detected in the unassembled sequence traces from the arachnid *Ixodes scapularis* nor in nematodes or vertebrates. The distribution of Mwh across distantly related arthropod orders suggested it was part of an ancient morphogenesis

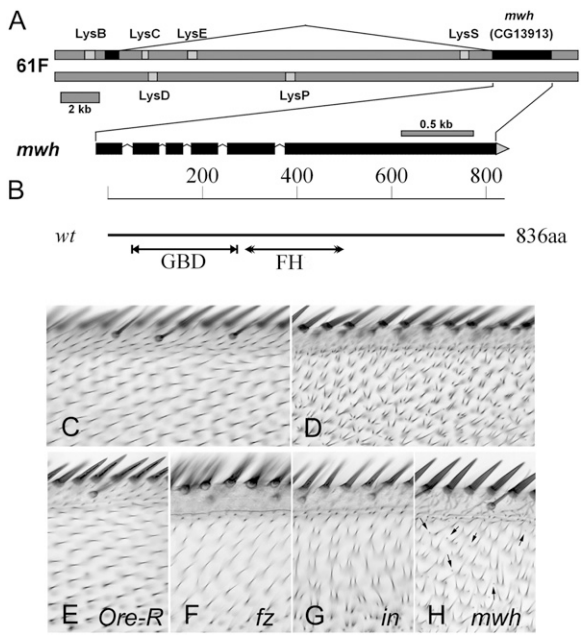

Figure 1.—The *mwh* gene and protein. (A) A representation of the *mwh* gene. Other genes in the region and the experimentally determined splicing pattern are shown. (B) A representation of the Mwh protein. The relative location of the GBD and FH3 domains are shown along the 836 amino acid protein. (C) The dorsal surface of the anterior edge of a *ap-Gal4/UAS-mwh; mwh* wing. (D) The ventral surface of the same wing. *ap-Gal4* drives expression of *mwh* only in dorsal cells providing rescue of the mutant phenotype in that cell layer. This rescue is seen in 100% of animals. (E–H) A small region from the anterior part of Ore-R, *fz*, *in*, and *mwh* wings. Note the hairs point distally in wild type but not in the mutants. The polarity phenotype is weaker in *fz* than *in* or *mwh* mutant wings in this region. Almost all of the cells in the *in* wing produce more than one hair and all of the cells in the *mwh* wing do so. One cell in the *fz* wing formed two hairs. The very small hairs seen in *mwh* wings (arrows) are not seen in any of the other genotypes.

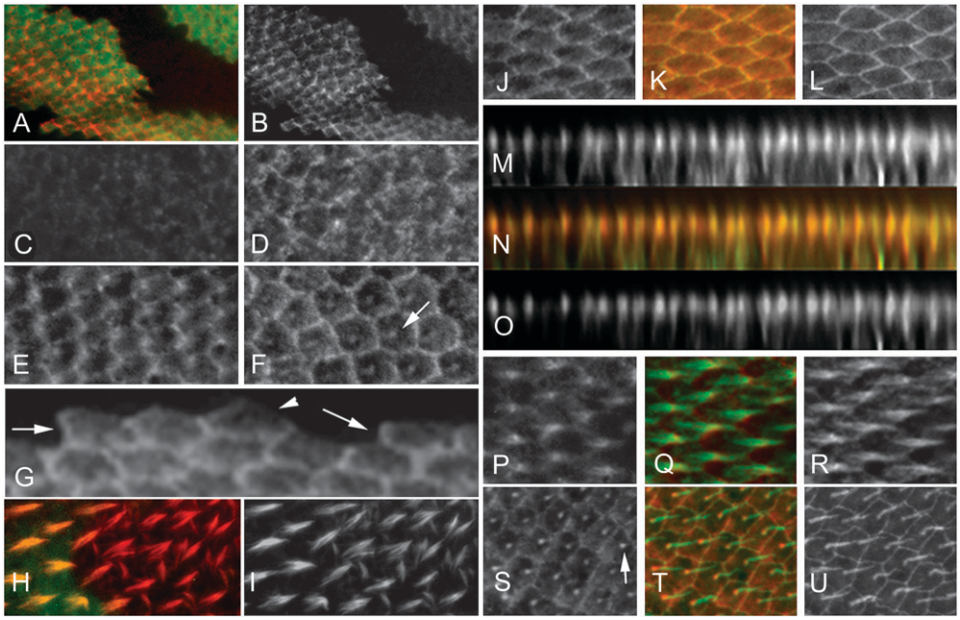

FIGURE 2.—Mwh localization is dynamic. (A and B) Confocal images of a *mwh* clone marked by a loss of GFP in a pupal wing stained with anti-GFP (green) and anti-Mwh (red) antibodies. A shows the merged image. B (as well as other single channel sections) is shown in grayscale as this provides better contrast. (C–F) Pupal wings stained with anti-Mwh antibody at 28 hr, 30 hr, 32 hr, and 36 hr after puparium formation (apf), respectively. The arrow points to accumulation of Mwh at the base of the hair in the 36-hr wing. (G) Mwh immunostaining at the boundary between expressing and nonexpressing cells. The arrows point to proximal edges that show accumulation of the protein. The arrowhead points to the distal edge of an expressing cell that does not accumulate Mwh. (H and I) A *mwh* clone marked by the loss of GFP and stained with phalloidin. Note the multiple hair cell phenotype is limited to the mutant cells. (J–L) Pupal wing cells stained with anti-Armadillo (green) and anti-Mwh (red) antibodies. K is a merge. (M–O) Z section reconstructions from the wing shown in J–L. Note that Mwh and Armadillo are colocalized near the apical surface of wing cells. (P–R) The accumulation of Mwh (red) and F-actin (green) in growing hairs. Note that Mwh is preferentially localized in proximal regions of the hair, but not extensively in the actin rootlet that extends into the cell. (S–U) Pupal wing cells aged ~36 hr apf. Note the accumulation of Mwh at the base of the hairs (arrow in G3).

network. Notable was the distinctive and highly conserved C-terminal KVTDLPSGLY motif. An FH3 domain was identified in our original Blast searches and additional psi-Blast searches and multiple sequence alignments (RIVERO *et al.* 2005) identified vertebrate genes that were similar to an ~430 amino acid region of Mwh that comprised the amino terminal regulatory region of Diaphanous family formins and included both GBD and FH3 domains (supplemental Figures S2 and S3). There are other Drosophila genes that are more similar to the identified vertebrate genes, thus, the vertebrate genes are not orthologs of *mwh*. Mwh does not contain the actin binding FH1 and FH2 domains that are characteristic of true formins, thus while related, Mwh is not a formin.

In the Diaphanous family formins the GBD domain binds a Rho GTPase and this displaces the autoinhibitory C-terminal DAD domain (WATANABE *et al.* 1999; ALBERTS 2001) from the DID. This leads to the activation of Diaphanous and its stimulation of actin polymerization. The residue changed in mwh^6 is within the GBD domain and conserved in other Mwhs. Hence this region is of functional significance. On the basis of similarity to Diaphanous, this residue is predicted to be part of the α-8 helix that interacts directly with the G protein (ROSE *et al.* 2005). By analogy, we suggest that the Mwh GBD domain will bind a small G protein in a regulatory interaction.

Mwh accumulation and localization is dynamic: We raised a polyclonal anti-Mwh antibody that was able to specifically detect the endogenous Mwh protein in pupal wings and used it to localize Mwh (Figure 2, A and B). We did not detect Mwh in wing disc or pupal wing cells by immunostaining prior to ~30 hr after puparium formation (apf) (Figure 2, C–F). By the time of hair initiation strong Mwh staining was detected.

As noted earlier we found only very weak rescue of *mwh* using *ptc-Gal4 UAS-mwh*. This could be due to *ptc-Gal4* not driving the needed level of *mwh* expression at the appropriate time. Consistent with this explanation we could easily detect a long stripe of Mwh by immunostaining of *ptc-Gal4; UAS-mwh* third instar wing discs and 24-hr pupal wings (supplemental Figure S4A). In 27-hr pupal wings Mwh staining was bright only in the center of the *ptc* domain (where *ptc-Gal4* activity is highest) in the proximal half of the wing (supplemental Figure S4B). In 32- to 34-hr apf pupal wings, during and after the start of hair growth we detected increased Mwh immunostaining only in very proximal regions in the center of the *ptc* domain (supplemental Figure S4, C and D). Using the decline in the intensity of staining we were able to follow the decline in Mwh levels and this allowed us to estimate that the half-life of the Mwh protein was at most 2–3 hr in young pupal wings (supplemental Figure S5).

We found a complex pattern for Mwh localization in pupal wing cells (Figure 2). Mwh accumulated in a zigzag pattern at the cell periphery of wing cells between 30 and 34 hr apf (Figure 2, E, and J–L). The accumulation was quite uneven. In z-sections it was located at

the same location as Armadillo (β-catenin), a key component of adherens junctions (Figure 2, M–O). Both the uneven zigzag staining and the accumulation near the adherens junctions are also properties of the PCP and PPE proteins. The Mwh staining pattern was not nearly as sharp as that seen with PCP proteins such as Stan or In as some Mwh was seen near but not at the proximal plasma membrane. Indeed, Mwh did not completely colocalize with Stan or In (Figure 3, A–F). The subcellular distribution of Mwh was dynamic. It accumulated in both emerging (*e.g.*, from 30 to 32 hr apf) (Figure 2E) and growing wing hairs (*e.g.*, from 32 to 34 hr apf) (Figure 2, F, and P–R). Compared to F-actin it appeared to accumulate preferentially in the proximal part of the hair. Later in hair morphogenesis Mwh preferentially localized to the base of the hairs (*e.g.*, after 36 hr apf) (Figure 2, F, and S–U). At later stages we also saw Mwh along the cell periphery, but the zigzag pattern was no longer distinct and the staining was relatively uniform. Other *fz* pathway proteins do not localize in growing hairs (Usui *et al.* 1999; Axelrod 2001; Strutt 2001; Tree *et al.* 2002; Bastock *et al.* 2003; Adler *et al.* 2004; Das *et al.* 2004).

To determine if Mwh was localized at the proximal or distal or both sides of cells, we immunostained pupal wings that contained *mwh* mutant clones. The staining pattern of cells located at clone boundaries showed that Mwh accumulated at the proximal sides of wing cells (Figure 2G). This pattern is also seen for Pk, Vang, and In.

The regulation of hair initiation and the actin cytoskeleton by *mwh*: *mwh* has long been used as a cuticular marker in genetic mosaics and thought to act cell autonomously. We confirmed this by examining marked clones in pupal wings where obvious changes in hair formation and the actin cytoskeleton were restricted to mutant cells (Figure 2, H and I).

The adult wing phenotype of *mwh* is similar to those of PCP and PPE genes in that loss-of-function mutations result in similar abnormal polarity phenotypes (Figure 1, E–H). For example, in a *fz*, *in*, or *mwh* mutant, hairs in the most anterior region of the wing point toward the anterior margin as opposed to distally as in wild type (Figure 1, E–H). In this region of the wing the *fz* phenotype is weaker than that of *in* or *mwh*. The *mwh* mutant phenotype differs from upstream genes due to most *mwh* cells forming three to five hairs instead of the one formed by the vast majority of *fz* cells and the one to three formed by *in* cells. Often, one or two of the hairs produced by a *mwh* cell were very small and such tiny hairs are rarely seen in mutants of PCP or PPE genes (Figure 1H).

That loss of *mwh* function led to extra hairs, suggested that Mwh served as an inhibitor to restrict hair initiation. However, the increase in *mwh* expression just prior to hair initiation suggested that Mwh might serve to activate the cytoskeleton. To attempt to distinguish between these hypotheses we examined the consequences of

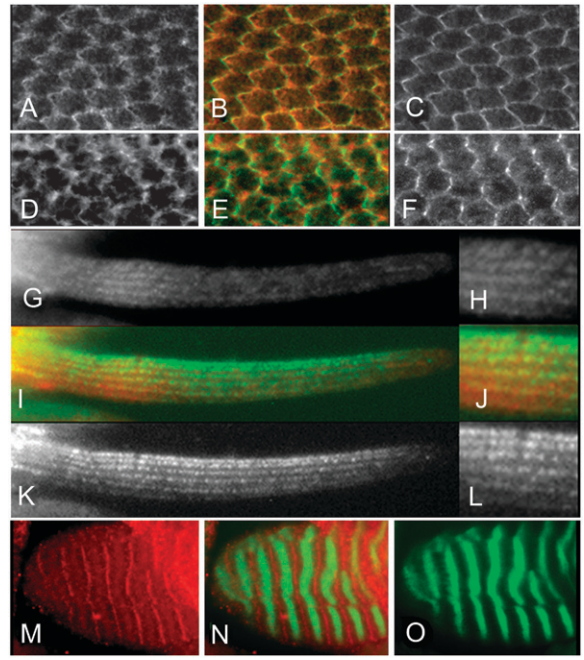

Figure 3.—(A–C) A 30-hr pupal wing stained with both anti-Mwh (red) and anti-Stan (green) antibodies. As in Figure 2 single-channel images are shown in grayscale to improve contrast. B is the merged image. Note the Stan staining is more precisely localized at the plasma membrane and the two proteins are not tightly colocalized. (D–F) A 30-hr pupal wing stained with both anti-Mwh (red) and anti-In (green) antibodies. In immunostaining is very sensitive to fixation so only very weak fixation was used in this experiment and this led to the poor anti-Mwh staining. (I and K) A wing bristle where the endogenous Mwh protein is immunostained (red). F-actin is in green. (J and L) Higher magnification images of the proximal region of the bristle. Note that Mwh accumulates along the large actin bundles and is preferentially in the proximal part of the bristle. M–O) A piece of larval body wall muscle where *mwh* expression was driven using Tubulin-Gal4. Mwh is shown in red and F-actin in green (Alexa 488 phalloidin). Note the strong Mwh staining in the gap between regions of F-actin staining.

expressing *mwh* precociously. We saw no change in the actin cytoskeleton in wing discs expressing *mwh* and we saw no change in the timing of hair initiation or the appearance of the cytoskeleton in pupal wings where *mwh* was precociously expressed by *ptc-Gal4*. Thus, Mwh did not show any evidence of activating hair initiation. A limitation of this experiment is that as noted earlier, at the normal time of hair initiation *ptc-Gal4* activity is low and does not result in *mwh* overexpression. To get around this limitation we directed a higher level of Mwh expression by using a combination of two Gal4 drivers (*e.g.*, *ptc-Gal4/+*; *Tub-Gal4/UAS-mwh*). In such flies, we observed a weak gain-of-function phenotype that consisted of occasional small hairs, cells that failed to form a hair, multiple hair cells, and regions of slightly altered polarity (Figure 4, A and B). These phenotypes were primarily seen in the proximal part of the *ptc* domain, in the vicinity of the posterior cross vein and in the

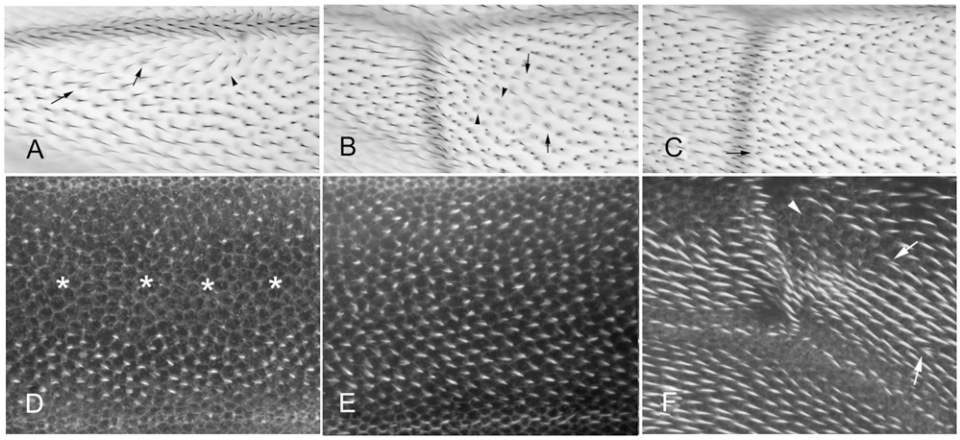

FIGURE 4.—The overexpression of *mwh* inhibits hair initiation. A and B are from *ptc-GAL4/+*; *Tub-Gal4/UAS-mwh* flies. A is from the dorsal wing surface just distal to the anterior cross vein. Several double hair cells are shown (arrows) and a weak polarity phenotype is seen. B is from the ventral surface just distal to the posterior cross vein. In this region many cells from very small hairs (or no hairs) (arrowheads) and others form double hair cells (arrows). (C) From a *ptc-GAL4/+*; *Tub-GAL4/+* fly. A high level of GAL4 expression can induce the formation of a small number of multiple hair cells (arrow). This phenotype is much weaker than that seen with *ptc-GAL4/+*; *Tub-Gal4/UAS-mwh* wings. The number of multiple hair cells is about fourfold higher in this latter genotype. (D) A *ptc-GAL4/+*; *Tub-Gal4/UAS-mwh* pupal wing stained for F-actin. (E) An equivalent Ore-R control wing. They are centered on the middle of the *ptc* domain ventral surface. Note the delayed hair formation in the central part of the *ptc* domain in D (marked with an asterisk). (F) A *ptc-GAL4/+*; *Tub-Gal4/UAS-mwh* showing the region around the posterior cross vein. Arrows point to cells forming multiple hairs. The arrowhead points to a cell that has not yet begun to form a hair.

proximal part of the anteriormost region of the wing. This phenotype while weak showed complete penetrance. In 32-hr pupal wings of this genotype we observed that hair initiation was delayed over a substantial part of the *ptc* domain and also near the posterior cross vein (Figure 4, D–F). Since the adult phenotype was seen in a much smaller region of the wing than the pupal phenotype we concluded that most of the cells that were delayed in hair initiation still produced adult hairs of normal morphology. The ability of cells with delayed hair initiation to "catch up" and produce normal adult hairs was previously seen for clones of *not* (*non-stop*) (REN *et al.* 2005). We concluded that Mwh acted as a negative regulator of hair initiation. The lack of an actin phenotype when overexpressed in wing discs or in loss-of-function mutations in many cell types (data not shown) indicated that Mwh was not a general regulator of the cytoskeleton, but rather a cell type/developmental stage-specific regulator.

The multiple hair cell phenotype and the accumulation of Mwh in growing hairs suggested that Mwh might bind to the actin cytoskeleton. To test this possibility we examined the distribution of Mwh in other cell types. *mwh* mutations do not result in a mutant phenotype in bristles, however by immunostaining we found the endogenous protein colocalized with the large bundles of actin filaments found around the periphery of growing bristles (Figure 3, G–L) (TILNEY *et al.* 1995). We extended these experiments to look at the localization of Mwh in larval body muscle and salivary gland cells where it is not normally expressed. The well-characterized sarcomeric structure of larval body wall muscle provided a scaffold to test the hypothesis that Mwh could bind to F-actin as opposed to an alternative cytoskeletal component. In larval muscle Mwh accumulated in a striated pattern (Figure 3, M–O) that did not coincide with F-actin staining and instead appeared to be localized to the M line. This suggested the possibility that Mwh interacted with a protein that regulated the activity or assembly of myosin. The lateral membranes of salivary gland cells stained strongly for F-actin and there were also bright staining actin "bars" in the basalmost one-third of these cells. When we expressed *mwh* in salivary gland cells, Mwh also accumulated at both of these locations (data not shown). We concluded that Mwh could bind to a constituent of the actin cytoskeleton but likely not F-actin itself.

***mwh* has two temporally separate functions:** The two locations for Mwh accumulation were temporally distinct suggesting they reflected separate functions. We used a series of temperature shifts with the temperature-sensitive mwh^6 allele to test this hypothesis. When mwh^6 flies were grown at 18° they showed only a very weak phenotype (Figure 5A). In contrast when grown at 29° they showed a strong hypomorphic phenotype (Figure 5D).

To facilitate the interpretation of shift experiments we first examined the timing of hair initiation in this stock at the permissive and restrictive temperatures. When this stock was grown at 29° we found 0 of 4 24-hr apf wings contained hairs, 3 of 5 27-hr apf wings contained hairs (when detected the hairs were quite short and were not seen in the proximalmost part of the wing), and 5 of 5 31-hr apf wings contained long hairs. We concluded that hair initiation was ~27 hr apf at 29°. When the stock was grown at 18°, 0 of 5 64-hr wings had hairs, 6 of 7 68- to 69-hr apf wings had hairs (in 5 of the 6 the hairs were short) and 13 of 13 70- to 72-hr apf wings had hairs (for 12/13 medium-length hairs were seen in all regions of the wing (see Figure 5, M and N). We concluded that hair initiation was ~67–69 hr apf at 18°.

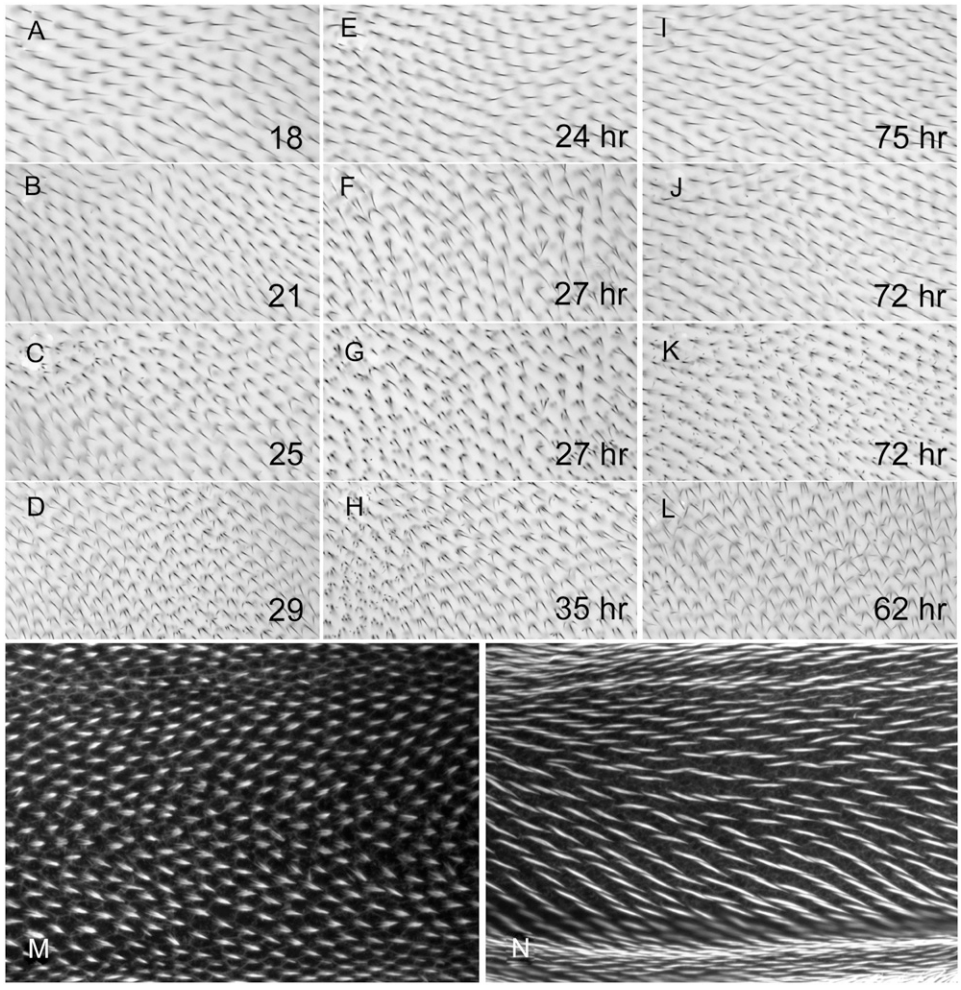

FIGURE 5.—*mwh* has two functions. (A–L) *mwh*^{6} adult wings after various temperature regimes. A–D are wings from flies raised completely at 18°, 21°, 25°, and 29°, respectively. Note how the phenotype becomes more severe as the temperature increased. E–H show wings from pupae that were shifted from 29° to 18° at 24 hr, 27 hr (shown at two focal planes), and 35 hr apf, respectively. Note that a shift at 27 hr produces a relatively strong polarity phenotype but only a small number of short hairs. I–L show wings from pupae shifted from 18° to 29° at 75 hr, 72 hr (two focal planes), and 62 hr apf. Note the many very small hairs in K. (M and N) *mwh*^{6} 70-hr pupal wings that show short- and medium-length hairs (as discussed in the text).

Initial temperature-shift experiments showed that the temperature-sensitive period was around the time of hair initiation.

To analyze the phenotypes of adult wings we examined qualitatively the polarity of hairs in the adult wing (Figure 5), and quantitatively the fraction of cells that formed a single hair and the average number of medium and long hairs per cell (within our test region) (Table 2). When pupae raised at the restrictive temperature (29°) were shifted to the permissive temperature (18°) prior to hair initiation (at 24 hr apf) the phenotype was indistinguishable from those grown continually at 18° (Figure 5, A and E). This was true for the abnormal polarity of hairs, the fraction of cells that formed a single hair (100%), and the average number of hairs/cell (1 per cell) (Table 2). When the shift was made a few hours later (27 hr apf, around the time of hair initiation), the wings were different from those grown entirely at either the permissive or restrictive temperature. They showed a moderate hair-polarity phenotype (Figure 5, F and G); 51% of cells formed a single hair and on average 1.63 hairs per cell (Table 2). There were few of the very small hairs that are common in *mwh* but not in *fy* or *frtz* mutants. When pupae were shifted several hours after hair formation (35 hr apf) there was no rescue and the wings resembled those from animals that were kept at 29°. They showed a strong polarity phenotype, only 4% of the cells formed a single hair and on average they contained 2.56 hairs per cell (Figure 5H and Table 2). Different results were seen with the complementary shifts. Shifting from 18° to 29° well after hair formation (75 hr apf) had no effect (Figure 5I and Table 2), while shifting pupae several hours prior to hair initiation (62/64 hr apf) resulted in a completely restrictive phenotype (Figure 5L and Table 2). Once again an intermediate phenotype was seen when pupae were shifted right around the time of hair initiation (68 hr apf) (Table 2). A novel result was obtained when animals were shifted several (≈4) hours after hair initiation (72 hr apf). With this shift most wing cells produced a single relatively normal length distally pointing hair (Figure 5J and Table 2). These phenotypes were similar to those seen when no shift was made. In addition, most of these cells produced several very small secondary hairs that could best be seen when the microscope was focused close to the surface of the wing (Figure 5K). We concluded from these observations that *mwh* functioned prior to hair initiation to control the

TABLE 2

Effects of temperature shifts on the phenotype of *mwh*^{ts}

Allele	Original temperature	Time of shift[a]	Fraction of single-hair cells[b]	P *vs.* 18°	P *vs.* 29°	Mean hairs/cell[c]	P *vs.* 18°	P *vs.* 29°
mwh^{ts}	18°	None	1.00 (0)	NR	0.002	1.00 (0.002)	NR	<0.001
mwh^{ts}	21°	None	0.87 (0.013)	0.005	0.002	1.14 (0.014)	<0.001	<0.001
mwh^{ts}	29°	None	0.055 (0.015)	0.002	NR	2.47 (0.028)	<0.001	NR
mwh^{ts}	18°	72 hr	1.00 (0)	1.00	0.002	1.00 (0.002)	1.0	<0.001
mwh^{ts}	18°	69 hr	1.00 (0)	1.00	0.002	1.00 (0.002)	1.0	<0.001
mwh^{ts}	18°	68 hr	0.78 (0.095)	0.015	0.002	1.26 (0.022)	<0.001	<0.001
mwh^{ts}	18°	66 hr	0.052 (0.0095)	0.002	0.699	2.48 (0.029)	<0.001	0.94
mwh^{ts}	29°	24 hr	1.00 (0)	1.00	0.002	1.00 (0.002)	1.0	<0.001
mwh^{ts}	29°	25 hr	0.995 (0.0034)	0.394	0.002	1.01 (0.0033)	0.842	<0.001
mwh^{ts}	29°	27 hr	0.51 (0.14)	0.015	0.002	1.63 (0.030)	<0.001	<0.001
mwh^{ts}	29°	31 hr	0.043 (0.011)	0.002	0.55	2.53 (0.0285)	<0.001	0.09
mwh^{1}	21°	None	0.012 (0.0048)	0.002	0.041	2.78 (0.030)	<0.001	<0.001

P, probability; NR, not relevant.

[a] Animals were shifted either from 18° to 29° or from 29° to 18°.

[b] The fraction of cells from our assay region forming a single hair was determined for six wings of each genotype and these values were compared. Only long- and medium-length hairs were considered. The Mann–Whitney rank sum test was used to test for significance, as the data points did not show equal variance.

[c] The distribution of hair-cell types (single, double, etc.) was determined for 100 cells from each of six wings. The 600 hair-cell populations from each genotype were compared. Only long- and medium-length hairs were considered. The Mann–Whitney rank sum test was used to test for significance, as the data points did not show equal variance.

number and polarity of medium/long hairs and after hair initiation to block the formation of small extra hairs. *mwh* is unique among *fz* pathway genes in having a function in the wing after hair initiation. Shifting temperature-sensitive alleles of *fz* or *in* after the time of hair initiation had no effect on hair number or polarity (Adler *et al.* 1994a,b). Further, inducing the expression of *fz* pathway components after hair initiation also failed to alter hair number or polarity (Krasnow and Adler 1994; Strutt and Strutt 2002, 2007).

DISCUSSION

***mwh* has two functions in hair morphogenesis:** The subcellular localization of Mwh was dynamic and unique for a protein involved in PCP. Mwh preferentially localized to the proximal side of pupal wing cells prior to hair formation (*e.g.*, 30–32 hr apf), in emerging hairs (at 32–34 hr), and later at the base of mature hairs (*e.g.*, after 36 hr apf) (Figure 2). Our temperature-shift experiments argued that *mwh* had discrete functions before and after hair initiation. We hypothesize that the early proximal accumulation of Mwh leads to hair initiation at the distal side of wing cells. This likely represents *mwh*'s function as a downstream component in the *fz* pathway. We further suggest that the inhibition of small ectopic hair formation that was detected by temperature shifts after hair initiation is mediated by Mwh that accumulates in the growing hair and in the base of the hair.

Our observation that the overexpression of *mwh* around the time of hair initiation can lead to a delay in hair initiation and a small and multiple hair phenotype in adult wings argues that Mwh acts as a negative regulator of hair initiation. This is consistent with Mwh being localized to the proximal side of wing cells when hairs initiate on the distal side, and Mwh being localized to the hair when it functions to prevent the formation of small hairs after the normal hair has begun to grow.

How is Mwh recruited to the hair? The accumulation of Mwh in the hair is presumably due to its interacting with one or more hair components. The hair contains both peripheral actin filaments and centrally localized microtubules. Because of the small size of the hair it is difficult to distinguish between Mwh accumulating with either or both of these cytoskeletons. We therefore examined the localization of Mwh in other cell types. In both bristles and salivary gland cells we found that Mwh colocalized with the actin cytoskeleton. Although Mwh contained a GBD–FH3 domain that is also found in formins it lacked the FH1 and FH2 domains that mediate formin binding to F-actin (Goode and Eck 2007). This suggested Mwh would not interact directly with actin. Consistent with this hypothesis we found that in larval muscle Mwh accumulated in a striated pattern that was offset from the bands of F-actin. From this we concluded that Mwh did not bind directly to F-actin. The localization to what appeared to be the M line in muscle suggested Mwh interacted with a protein that regulated myosin assembly or activity in striated muscle (Mercer *et al.* 2006; Musa *et al.* 2006) and perhaps with a similar protein in epidermal cells.

Mwh, G proteins, and formins: The sequence similarity between Mwh and the regulatory domain of formins suggested several possible biochemical mechanisms that could be functionally important. In Diaphanous family formins the GBD binds Rho1, which results in the

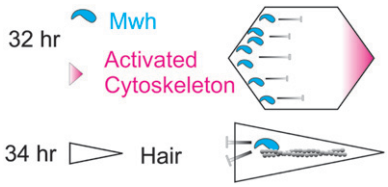

Figure 6.—A model for *mwh* function. In 32-hr pupal wings Mwh accumulates on the proximal side of wing cells. As differentiation proceeds, activators of the cytoskeleton accumulate. Local inhibition by Mwh leads to the cytoskeleton being activated in the distalmost part of the cell. In 34-hr pupal wings hair morphogenesis has begun. The growing hair contains both F-actin and microtubules and associated bound proteins. Mwh is recruited to the proximal part of the hair. At this location it inhibits the cytoskeleton from initiating new hair outgrowth centers.

activation of the formin to promote actin polymerization (Goode and Eck 2007). Rho1 has been implicated in fly planar polarity, making it a strong candidate for interacting with Mwh (Strutt *et al.* 1997). In preliminary studies we have obtained both genetic and biochemical evidence for such an interaction but the interpretation of the data is complicated by our finding that Rho1 has multiple functions in wing hair development. The presence of the DD domain also suggests the possibility that Mwh might dimerize with a true formin and regulate the actin cytoskeleton in that way. An obvious candidate for such a function is the DAAM formin, which in Xenopus was found to bind to Dsh (Habas *et al.* 2001). However, studies on fly DAAM failed to reveal any function in planar polarity or hair morphogenesis (Matusek *et al.* 2006). The *diaphanous* gene is another potential candidate. This gene has been well studied but there are no reports on its role in the differentiation of the adult epidermis. Intriguingly, Diaphanous localizes to growing embryonic denticles (Price *et al.* 2006), which like hairs are actin-containing extensions of epidermal cells. As is the case for epidermal hairs, *mwh* mutations result in the formation of extra denticles (Dickinson and Thatcher 1997) suggesting Dia as a possible partner for Mwh. None of the other fly formins have been found to function in wing hair development or wing planar polarity but several have not been well studied and are expressed in pupal wings (*e.g.*, CG10990, Formin 3, and Fhos) (Ren *et al.* 2005). One of these could function with *mwh*.

A model for Mwh in wing tissue polarity: There are several possible models as to how Mwh located on the proximal side of wing cells resulted in distal hair formation. One is that proximal Mwh stimulated hair initiation at the juxtaposed distal side of neighboring cells. However, *mwh* acts cell autonomously so we can rule out this model. An alternative is that Mwh, In and other PPE proteins formed a protein complex that organized the cytoskeleton to direct intracellular transport of hair-building components to the distal side leading to hair initiation there. This is plausible but no changes in the cytoskeleton prior to hair initiation have been seen in these mutants. A third possible model and one we prefer is that proximal Mwh locally inhibits hair initiation by regulating the cytoskeleton (Figure 6). This would lead to the preferential activation of the cytoskeleton on the distal side of the cell where Mwh levels were lowest. The cytoskeleton would self assemble to refine the area for hair initiation to a small region near the distal vertex. As the cytoskeleton is activated distally and a new hair emerges, Mwh would be recruited to this region, perhaps by binding to a hair component and/or a protein that interacted with a cellular myosin. Mwh would once again function locally to inhibit new hair initiation events and hence ensure that only a single unbranched hair forms. We view this latter Mwh function as a type of feedback inhibition that limits the activation of the cytoskeleton.

We gratefully acknowledge the provision of laboratory space by M. Ashburner. We thank Jeannette Charlton for technical help. The NCBI, EBI, FlyBase, and the Kyoto University GenomeNet supplied online bioinformatics services used in this study. We thank the reviewers for helpful comments. This work was supported by a grant from the National Institute of General Medical Science to P.N.A. and a grant from the United Kingdom Medical Research Council to Michael Ashburner.

LITERATURE CITED

Adler, P. N., 1992 The genetic control of tissue polarity in Drosophila. BioEssays **14:** 735–741.

Adler, P. N., J. Charlton, K. H. Jones and J. Liu, 1994a The cold-sensitive period for frizzled in the development of wing hair polarity ends prior to the start of hair morphogenesis. Mech. Dev. **46:** 101–107.

Adler, P. N., J. Charlton and W. J. Park, 1994b The Drosophila tissue polarity gene inturned functions prior to wing hair morphogenesis in the regulation of hair polarity and number. Genetics **137:** 829–836.

Adler, P. N., C. Zhu and D. Stone, 2004 Inturned localizes to the proximal side of wing cells under the instruction of upstream planar polarity proteins. Curr. Biol. **14:** 2046–2051.

Alberts, A. S., 2001 Identification of a carboxyl-terminal diaphanous-related formin homology protein autoregulatory domain. J. Biol. Chem. **276:** 2824–2830.

Axelrod, J. D., 2001 Unipolar membrane association of Dishevelled mediates Frizzled planar cell polarity signaling. Genes Dev. **15:** 1182–1187.

Bastock, R., H. Strutt and D. Strutt, 2003 Strabismus is asymmetrically localised and binds to Prickle and Dishevelled during Drosophila planar polarity patterning. Development **130:** 3007–3014.

Curtin, J. A., E. Quint, V. Tsipouri, R. M. Arkell, B. Cattanach *et al.*, 2003 Mutation of Celsr1 disrupts planar polarity of inner ear hair cells and causes severe neural tube defects in the mouse. Curr. Biol. **13:** 1129–1133.

Dabdoub, A., and M. W. Kelley, 2005 Planar cell polarity and a potential role for a Wnt morphogen gradient in stereociliary bundle orientation in the mammalian inner ear. J. Neurobiol. **64:** 446–457.

Das, G., A. Jenny, T. J. Klein, S. Eaton and M. Mlodzik, 2004 Diego interacts with Prickle and Strabismus/Van Gogh to localize planar cell polarity complexes. Development **131:** 4467–4476.

Dickinson, W. J., and J. W. Thatcher, 1997 Morphogenesis of denticles and hairs in Drosophila embryos: involvement of actin-associated proteins that also affect adult structures. Cell Motil. Cytoskeleton **38:** 9–21.

Feiguin, F., M. Hannus, M. Mlodzik and S. Eaton, 2001 The ankyrin repeat protein Diego mediates Frizzled-dependent planar polarization. Dev. Cell **1:** 93–101.

Goode, B. L., and M. J. Eck, 2007 Mechanisms and function of formins in the control of actin assembly. Ann. Rev. Biochem. **76:** 593–627.

Gubb, D., and A. García-Bellido, 1982 A genetic analysis of the determination of cuticular polarity during development in *Drosophila melanogaster*. J. Embryol. Exp. Morphol. **68:** 37–57.

Guo, N., C. Hawkins and J. Nathans, 2004 From the cover: Frizzled6 controls hair patterning in mice. Proc. Natl. Acad. Sci. USA **101:** 9277–9281.

Habas, R., Y. Kato and X. He, 2001 Wnt/Frizzled activation of Rho regulates vertebrate gastrulation and requires a novel formin homology protein Daam1. Cell **107:** 843–854.

Jessen, J. R., J. Topczewski, S. Bingham, D. S. Sepich, F. Marlow *et al.*, 2002 Zebrafish trilobite identifies new roles for Strabismus in gastrulation and neuronal movements. Nat. Cell Biol. **4:** 610–615.

Krasnow, R. E., and P. N. Adler, 1994 A single frizzled protein has a dual function in tissue polarity. Development **120:** 1883–1893.

Lawrence, P. A., G. Struhl and J. Casal, 2007 Planar cell polarity: One or two pathways? Nat. Rev. Genet. **8:** 555–563.

Lee, H., and P. N. Adler, 2002 The function of the frizzled pathway in the Drosophila wing is dependent on inturned and fuzzy. Genetics **160:** 1535–1547.

Matusek, T., A. Djiane, F. Jankovics, D. Brunner, M. Mlodzik *et al.*, 2006 The Drosophila formin DAAM regulates the tracheal cuticle pattern through organizing the actin cytoskeleton. Development **133:** 957–966.

Mercer, K. B., R. K. Miller, T. L. Tinley, S. Sheth, H. Qadota *et al.*, 2006 Caenorhabditis elegans UNC-96 is a new component of M-lines that interacts with UNC-98 and paramyosin and is required in adult muscle for assembly and/or maintenance of thick filaments. Mol. Biol. Cell **17:** 3832–3847.

Montcouquiol, M., E. B. Crenshaw and M. W. Kelley, 2006 Noncanonical Wnt signaling and neural polarity. Annu. Rev. Neurosci. **29:** 363–386.

Musa, H., S. Meek, M. Gautel, D. Peddie, A. J. Smith *et al.*, 2006 Targeted homozygous deletion of M-band titin in cardiomyocytes prevents sarcomere formation. J. Cell Sci. **119:** 4322–4331.

Price, M. H., D. M. Roberts, B. M. McCartney, E. Jezuit and M. Peifer, 2006 Cytoskeletal dynamics and cell signaling during planar polarity establishment in the Drosophila embryonic denticle. J. Cell Sci. **119:** 403–415.

Ren, N., C. Zhu, H. Lee and P. N. Adler, 2005 Gene expression during Drosophila wing morphogenesis and differentiation. Genetics **171:** 625–638.

Rivero, F., T. Muramoto, A.-K. Meyer, H. Urushihara, T. Uyeda *et al.*, 2005 A comparative sequence analysis reveals a common GBD/FH3–FH1-FH2-DAD architecture in formins from Dictyostelium, fungi and metazoa. BMC Genomics **6:** 28.

Rose, R., M. Weyand, M. Lammers, T. Ishizaki, M. R. Ahmadian *et al.*, 2005 Structural and mechanistic insights into the interaction between Rho and mammalian Dia. Nature **435:** 513–518.

Strutt, D., and H. Strutt, 2007 Differential activities of the core planar polarity proteins during Drosophila wing patterning. Dev. Biol. **302:** 181–194.

Strutt, D. I., 2001 Asymmetric localization of Frizzled and the establishment of cell polarity in the Drosophila wing. Mol. Cell **7:** 367–375.

Strutt, D. I., U. Weber and M. Mlodzik, 1997 The role of RhoA in tissue polarity and Frizzled signalling. Nature **387:** 292–295.

Strutt, H., and D. Strutt, 2002 Nonautonomous planar polarity patterning in Drosophila: dishevelled-independent functions of frizzled. Dev. Cell **3:** 851–863.

Taylor, J., N. Abramova, J. Charlton and P. N. Adler, 1998 Van Gogh: a new Drosophila tissue polarity gene. Genetics **150:** 199–210.

Tilney, L., M. Tilney and G. Guild, 1995 F actin bundles in Drosophila bristles. I. Two filament cross-links are involved in bundling. J. Cell Biol. **130:** 629–638.

Tree, D. R. P., J. M. Shulman, R. Rousset, M. P. Scott, D. Gubb *et al.*, 2002 Prickle mediates feedback amplification to generate asymmetric planar cell polarity signaling. Cell **109:** 371–381.

Usui, T., Y. Shima, Y. Shimada, S. Hirano, R. W. Burgess *et al.*, 1999 Flamingo, a seven-pass transmembrane cadherin, regulates planar cell polarity under the control of Frizzled. Cell **98:** 585–595.

Vinson, C. R., and P. N. Adler, 1987 Directional non-cell autonomy and the transmission of polarity information by the frizzled gene of Drosophila. Nature **329:** 549–551.

Wallingford, J. B., S. E. Fraser and R. M. Harland, 2002 Convergent extension: the molecular control of polarized cell movement during embryonic development. Dev. Cell **2:** 695–706.

Wang, Y., N. Guo and J. Nathans, 2006 The role of Frizzled3 and Frizzled6 in neural tube closure and in the planar polarity of inner-ear sensory hair cells. J. Neurosci. **26:** 2147–2156.

Watanabe, N., T. Kato, A. Fujita, T. Ishizaki and S. Narumiya, 1999 Cooperation between mDia1 and ROCK in Rho-induced actin reorganization. Nat. Cell Biol. **1:** 136–143.

Wong, L., and P. Adler, 1993 Tissue polarity genes of Drosophila regulate the subcellular location for prehair initiation in pupal wing cells. J. Cell Biol. **123:** 209–221.

Ybot-Gonzalez, P., D. Savery, D. Gerrelli, M. Signore, C. E. Mitchell *et al.*, 2007 Convergent extension, planar-cell-polarity signalling and initiation of mouse neural tube closure. Development **134:** 789–799.

Communicating editor: J. A. Lopez